RSC Advances

PAPER

Cite this: *RSC Adv.*, 2022, **12**, 648

Anisotropic Kubo conductivity of electric field-induced monolayer β_{12}-borophene

Mohammad Mortezaei Nobahari

Received 28th October 2021
Accepted 3rd December 2021

DOI: 10.1039/d1ra07945j

rsc.li/rsc-advances

In this paper, we used three monolayer β_{12}-borophene Hamiltonian models to calculate the band structure, intra-band, and inter-band optical conductivity (IOC). Linear response theory and the Kubo formula are employed to calculate optical conductivity. We have shown that the band gap proportional to the inversion non-symmetric model increases by applying an external electric field (EEF), and for homogeneous and inversion-symmetric models, gap opening occurs. We found an anisotropic behavior in the IOC of β_{12}-borophene for polarized light along x and y-directions. The peak of the real part of the IOC for polarized light along the x-direction ($\Re\sigma_{xx}$) locates at the energy equal to the band gap and by applying an EEF shifts to the higher energies and experiences a blue shift. Also, the electric field has little effect on the IOC along y-direction (σ_{yy}) and in contrast to σ_{xx}, by applying an electric field, the peak of the IOC shifts towards lower energies and a redshift occurs. In addition, unlike inter-band transitions, the intra-band optical conductivity of β_{12}-borophene is isotropic in all three models, and an EEF can not shift plots to higher or lower energies and only reduces the height of both imaginary and real parts of the optical conductivity.

1 Introduction

After the synthesis of graphene in 2004, two-dimensional (2D) materials attracted the attention of researchers.[1] This work opened up a new window for researching low-dimensional materials. Due to its zero band gap and low on/off ratio, researchers looked for new alternative materials. To date, there are more than 700 stable 2D materials like phosphorene, silicon, borophene,.*etc.* In recent years, several types of borophene were synthesized on the Ag(111) substrate.[2–4] There are many types of borophene, but due to the strong interaction between β_{12} and the Ag substrate, this material is one of the most stable boron allotropes.[5,6] Other allotropes of boron are not as stable as β_{12}-borophene.[7] By using chemical bonding analyses based on the adaptive natural density partitioning (AdNDP) method, it understood that all 2D boron clusters have an outer ring featuring strong two-center, two-electron (2c-2e) B–B bonds (in which two valence electrons are shared between two atoms) and other atoms interacting with the peripheral ring almost exclusively through delocalized σ and π bonding.[8,9] The main challenge in 2D materials is their instability. However, researchers are trying to overcome this by using an appropriate substrate, but the difference between lattice parameters of the substrate and two-dimensional material can make it unstable.[10] Borophene, due to its electron mobility, band gap, and anisotropic properties and having both a massless Dirac fermion and massless/massive triplet fermions[11,12] is different from other 2D materials. Researchers observed the Dirac fermions in β_{12}-borophene by angle-resolved photoemission spectroscopy, a tight-binding model and first-principles calculations.[11–14] The results indicated that β_{12} is particularly metallic.[15–19] It is understood that lattice thermal conductance in the ballistic regime of borophene is very high and similar to graphene in low frequencies, phonons transition in borophene is almost isotropic, and for high frequencies, phonon transition is one-dimensional, and phonons move in one direction.[20] Also, it is understood that borophene behaves like a superconductor in the critical temperature range of $T_c \simeq 10$–20 K since it has a small atomic mass.[21] Using non-equilibrium Green's function simulations and first-principles calculations, thermal conductance of the borophene monolayer has been calculated.[20] In a study by Kistanov *et al*[22] charge localization, and the band gap opening of borophene were studied using the first-principles method. The mechanical properties of borophene are unique because of its anisotropic structure. In a study by Mannix *et al*[2] The Young's modulus of borophene was calculated in special directions. It was found that this quantity in the k_x-direction is 398 GPa nm which is even greater than graphene, so it is one of the hardest 2D materials. Effects of the electric field and the charged impurity on the electronic phase and electrical conductivity of β_{12}-borophene were studied using linear response theory and a Green's function approach.[23] Using density functional theory (DFT) researchers studied strain effects on the optical absorbance and electronic band structure of β_{12} and δ_6.[24] Also, Zhang *et al*[25] have predicted the high potential of β_{12} and χ_3 phases of borophene for Li-ion and Na-ion batteries. Based on DFT calculations, the electronic, optical, and thermodynamic features of striped borophene were calculated by Peng *et al.*[26]

Department of Sciences, Ferdowsi University of Mashhad, Iran. E-mail: mortezaie.mm71@gmail.com

Optical conductivity is one of the most significant properties of the materials that describes the material's response to electromagnetic waves. Knowing the optical conductivity of materials help us to understand the pattern of absorption and scattering of the incident light, and these parameters are critical for use in solar cell technology and optoelectronics. Absorption and scattering are controllable in different ways. Potential gates are one of these methods. Applying an electric field to the β_{12}-borophene generates on-site energies, thus increasing the gap and changing the absorption and scattering pattern.

Due to the inability to solve the 5×5 β_{12}-borophene Hamiltonian analytically, to date, there is no report of calculating the optical conductivity of β_{12}-borophene using the tight-binding approximation and Kubo formula. According to the Kubo formula, we need both eigenvalues and eigenvectors of the 5×5 Hamiltonian to calculate the optical conductivity. For this purpose, in the present work, we will use a numerical method to diagonalize the Hamiltonian and calculate direction-dependent velocities and optical conductivity.

By considering different symmetries for on-site energies and hopping parameters, there are three various Hamiltonian models of β_{12}-borophene.[11] The symmetries of the β_{12}-borophene lattice are the inversion symmetry model, but this symmetry can be broken due to the Ag substrate, and this leads to the inversion non-symmetric model. The third model is called the homogeneous model. In this model, all hopping parameters and on-site energies are equal, and some features of β_{12}-borophene are present only in this model (*e.g.* gapless triplet fermions).

In this paper, we will investigate the intra-band and inter-band optical conductivity of β_{12}-borophene using linear response theory and the Kubo formula and study the EEF effects on the optical conductivity along the x (σ_{xx}) and y (σ_{yy}) directions. For this purpose, first, we will calculate the band structure of β_{12}-borophene, then focus on the high symmetry points K and K' (band gap) to interpret the EEF effects on the IOC. We will also calculate the intra-band optical conductivity and study the EEF effects on the imaginary and real parts.

2 Theory

β_{12}-borophene has a honeycomb lattice structure with five atoms in its unit cell. Atoms are labeled as a, b, c, d, and e as illustrated in Fig. 1. The unit cell has length $a = 2.923\ 6$ Å and width $b = \sqrt{3}a$ Å, which is one-half of the honeycomb lattice. The first Brillouin zone of β_{12} is a rectangle with $-\pi/a \le k_x \le \pi/a$ and $-\pi/b \le k_y \le \pi/b$ however, we can shift the first Brillouin zone in the k_x-direction and use $0 \le k_x \le 2\pi/a$. Using the tight-binding approximation, the β_{12}-borophene Hamiltonian is

$$H = \begin{pmatrix} \varepsilon_a & t_{ab}g & t_{ac}f^* & 0 & t_{ae}f \\ t_{ab}g^* & \varepsilon_b & t_{bc}g & t_{bd}f^* & 0 \\ t_{ac}f & t_{bc}g^* & \varepsilon_c & t_{cd}g & t_{ce}f^* \\ 0 & t_{bd}f & t_{cd}g^* & \varepsilon_d & t_{de}g \\ t_{ae}f^* & 0 & t_{ce}f & t_{de}g^* & \varepsilon_e \end{pmatrix}, \quad (1)$$

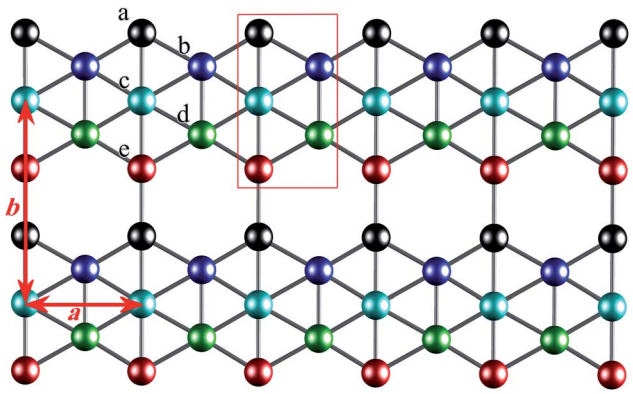

Fig. 1 Top view of the geometry structure of β_{12} borophene. Atoms are labeled as a, b, c, d and e in different colors. The unit cell is presented by the red solid lines in the rectangle shape.

where $f = \exp(iak_y/\sqrt{3})$ and $g = 2\exp(-iak_y/2\sqrt{3})\cos(ak_x/2)$. According to the different symmetries for on-site energies and hopping parameters, there are three Hamiltonian models with different on-site energies and hopping parameters[11] which are known as:

inversion non-symmetric with

$$\varepsilon_a = \varepsilon_d = 0.196 \text{ eV}, \varepsilon_b = \varepsilon_e = -0.058 \text{ eV}, \varepsilon_c = -0.845 \text{ eV}, \quad (2)$$

$$t_{ab} = t_{de} = -2.04 \text{ eV}, t_{ac} = t_{ce} = -1.79 \text{ eV}, t_{bc} = t_{cd} = -1.84 \text{ eV}, t_{ae} = -2.12 \text{ eV}, t_{bd} = -1.91 \text{ eV}; \quad (3)$$

inversion symmetric with

$$\varepsilon_a = \varepsilon_e = 0.196 \text{ eV}, \varepsilon_b = \varepsilon_d = -0.058 \text{ eV}, \varepsilon_c = -0.845 \text{ eV}, \quad (4)$$

$$t_{ab} = t_{de} = -2.04 \text{ eV}, t_{ac} = t_{ce} = -1.79 \text{ eV}, t_{bc} = t_{cd} = -1.84 \text{ eV}, t_{ae} = -2.12 \text{ eV}, t_{bd} = -1.91 \text{ eV}; \quad (5)$$

and the homogeneous model with $t_{ij} = t = -2$ eV and zero on-site energies ($\varepsilon_i = 0$).

Fig. 2 presents the band structure of the homogeneous model. High symmetry points K' and K reflect Dirac fermions at zero energy ($\varepsilon = 0$) with positions $K' = (-2\pi/3a, 0)$ and $K = (2\pi/$

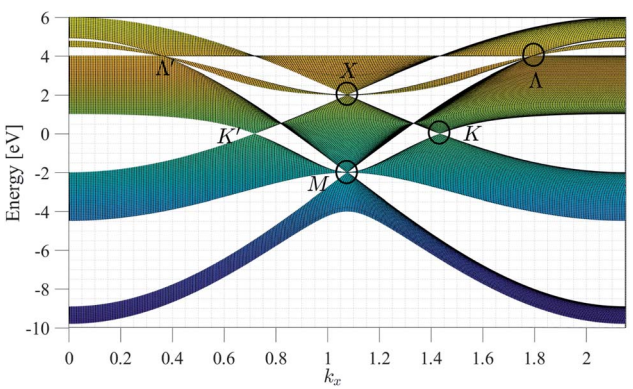

Fig. 2 Band structure of β_{12}-borophene for the homogeneous model.

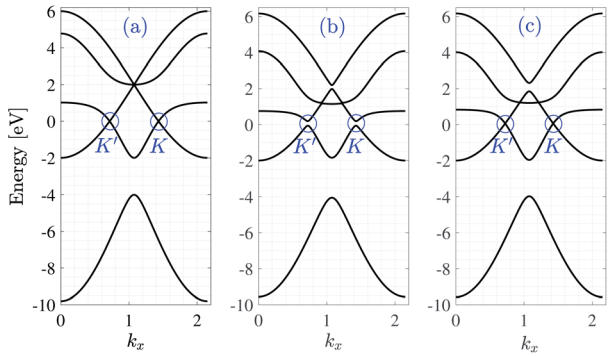

Fig. 3 Band structure of β_{12}-borophene for the (a) homogeneous (b) inversion non-symmetric and (c) inversion symmetric models.

$3a$, 0) and X and M points are triplet fermions at the non-zero energies and the three-band touching point Λ. As is clear in Fig. 2, β_{12}-borophene has five bands including two valences and three conduction bands with a direct gap that varied for different Hamiltonian models. Fig. 3 shows the band structure of the homogeneous, inversion symmetric, and inversion non-symmetric Hamiltonian models. It is clear that proportional band gaps (at K or K') for the homogeneous and inversion-symmetric models are zero, but in the inversion non-symmetric model, there is a gap of about $\simeq 0.254$ eV.[11]

2.1 Optical conductivity

In general, Ohm's law is $J = \sigma E$ where J is the current density, E is the electric field, and σ is the optical conductivity tensor

$$\sigma = \begin{pmatrix} \sigma_{xx} & \sigma_{xy} \\ \sigma_{yx} & \sigma_{yy} \end{pmatrix}. \tag{6}$$

For calculating the optical conductivity of materials first we need current operator. The current operator definition is $j_\mu = e\partial H/\partial k_\mu$ where $\mu = x$ or y.

$$j_\mu = e\begin{pmatrix} 0 & t_{ab}\frac{\partial g}{\partial k_\mu} & t_{ac}\frac{\partial f^*}{\partial k_\mu} & 0 & t_{ae}\frac{\partial f}{\partial k_\mu} \\ t_{ab}\frac{\partial g^*}{\partial k_\mu} & 0 & t_{bc}\frac{\partial g}{\partial k_\mu} & t_{bd}\frac{\partial f^*}{\partial k_\mu} & 0 \\ t_{ac}\frac{\partial f}{\partial k_\mu} & t_{bc}\frac{\partial g^*}{\partial k_\mu} & 0 & t_{cd}\frac{\partial g}{\partial k_\mu} & t_{ce}\frac{\partial f^*}{\partial k_\mu} \\ 0 & t_{bd}\frac{\partial f}{\partial k_\mu} & t_{cd}\frac{\partial g^*}{\partial k_\mu} & 0 & t_{de}\frac{\partial g}{\partial k_\mu} \\ t_{ae}\frac{\partial f^*}{\partial k_\mu} & 0 & t_{ce}\frac{\partial f}{\partial k_\mu} & t_{de}\frac{\partial g^*}{\partial k_\mu} & 0 \end{pmatrix}, \tag{7}$$

General form for the current operator is

$$j_\mu = -\frac{e}{\hbar}\Sigma_k c_k^\dagger c_k \alpha_k{}^\mu + i\frac{e}{\hbar}\Sigma_k c_k^\dagger c_k \beta_k{}^\mu, \tag{8}$$

where first term is related to the diamagnetic and the second term represents paramagnetic current. In eqn (8), e is the electron charge, $c_k^\dagger$ and c_k are annihilation and creation operators and α_k^μ and β_k^μ are intra-band and inter-band direction depended velocities in μ-direction respectively.

By using linear response theory, the optical conductivity is given as

$$\sigma_{\mu\mu'}(\omega) = \frac{g_s}{\hbar\omega S}\int \mathrm{d}t e^{i\omega t}\left\langle\left[j_\mu(t), j_{\mu'}(0)\right]\right\rangle, \tag{9}$$

where $g_s = 2$ is the spin degeneracy, ω is the photon frequency and S is the 2D planar area.

Using eqn (9), inter-band optical conductivity is given as[27,28]

$$\sigma^{\text{inter}}_{\mu\mu'}(\omega) = i\frac{g_s e^2}{\hbar^2\omega S}\sum_k\left(\beta_k{}^\mu\beta_k{}^{\mu'}\right)\left[\frac{f_{k,c}-f_{k,v}}{\hbar\omega+\Delta E+i\eta_1} - \frac{f_{k,c}-f_{k,v}}{\hbar\omega-\Delta E+i\eta_1}\right]. \tag{10}$$

where $f_{k,c}$, and $f_{k,v}$ are Fermi–Dirac distributions in the conduction and the valence bands respectively, η_1 is the finite damping between the conduction and the valence bands, and $\Delta E = E_c - E_v$ is the energy difference, where E_c and E_v are conduction and valence bands' energies respectively and $\beta_k{}^\mu = \langle k,c|j_\mu|k,v\rangle$ and $\beta_k{}^{\mu'} = \langle k,v|j_{\mu'}|k,c\rangle$ are velocities along the μ and μ'-directions.

For low-frequency photons in the THz region (between the microwave and infra-red), intra-band optical conductivity plays the main role in the optical conductivity. Inra-band transitions are between a special band and in eqn (10) c = v and $(f_{k,c}-f_{k,v})/\Delta E$ must be interpreted as $-\partial f(k)/\partial\varepsilon_j$ and Drude-like conductivity described as[29]

$$\sigma^{\text{intra}}_{\mu\mu'} = \frac{1}{S}\frac{ie^2\hbar}{\hbar\omega+i\eta_2}\sum_{k,j}\alpha_k{}^\mu\alpha_k{}^{\mu'}\left(\frac{-\partial f(k)}{\partial\varepsilon_j}\right). \tag{11}$$

Here $f(k) = 1/(1 + \exp((\varepsilon_j - \mu_0)/k_B T))$ is the Fermi–Dirac distribution, ε_j is jth eigenvalue, μ_0 is chemical potential, K_B is Boltzmann's constant, T is temperature and η_2 is the broadening width determined by scattering or disorder in the conduction band. In this paper, we considered $T = 10$ K.

For studying EEF effects on the β_{12}-borophene, we considered two voltage gates $V/2$ and $-V/2$ that are placed at the top and the bottom of β_{12}-borophene, respectively. The total Hamiltonian after perturbation by the electric field is

$$H = \begin{pmatrix} \varepsilon_a + V/2 & t_{ab}g & t_{ac}f^* & 0 & t_{ae}f \\ t_{ab}g^* & \varepsilon_b + V/2 & t_{bc}g & t_{bd}f^* & 0 \\ t_{ac}f & t_{bc}g^* & \varepsilon_c & t_{cd}g & t_{ce}f^* \\ 0 & t_{bd}f & t_{cd}g^* & \varepsilon_d - V/2 & t_{de}g \\ t_{ae}f^* & 0 & t_{ce}f & t_{de}g^* & \varepsilon_e - V/2 \end{pmatrix}. \tag{12}$$

where we considered zero contribution of c atoms. Using this Hamiltonian and eqn (10) and (11), we will be able to investigate EEF effects on the optical conductivity of β_{12}-borophene.

3 Results and discussion

The electronic phase plays an important role in the optical properties, and any change in the electronic phase affects

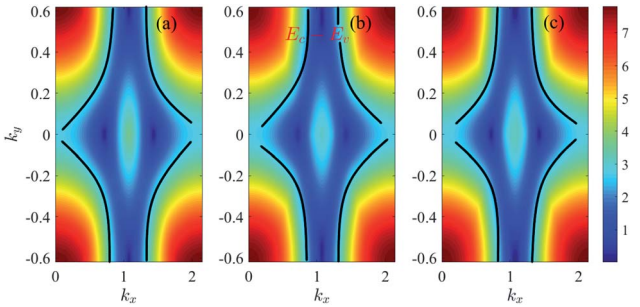

Fig. 4 Contour plots of energy difference between the lowest conduction band (E_c) and the highest valence band (E_v) in $-\pi/b \leq k_y \leq \pi/b$ and $0 \leq k_x \leq 2\pi/a$ for (a) homogeneous, (b) inversion non-symmetric and (c) inversion symmetric models. The black solid lines represent the maximum continuous equal energy in a Brillouin zone. The color bar represents the energy difference value.

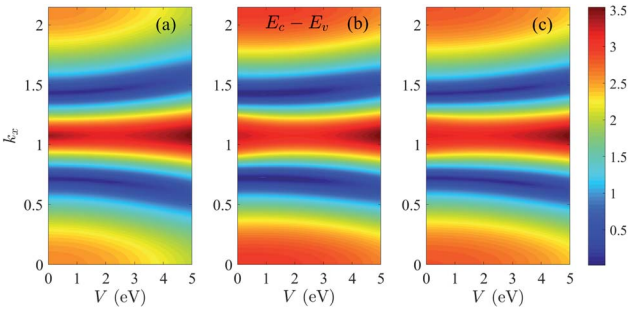

Fig. 6 Contour plots of energy difference between the lowest conduction band (E_c) and the highest valence band (E_v) for different voltages in $k_y = 0$ and $0 \leq k_x \leq 2\pi/a$ for (a) homogeneous, (b) inversion non-symmetric and (c) inversion symmetric models.

optical properties. Fig. 4 shows the energy difference between the highest valence and the lowest conduction bands for $-\pi/b \leq k_y \leq \pi/b$ and $0 \leq k_x \leq 2\pi/a$ at zero EEF. The solid black lines represent the maximum equal energy difference between the lowest conduction and highest valence bands. When the equal energy difference in Fig. 4 is continuous, it is easy for carriers in the valence band to absorb photon energy and transfer it to the conduction band. However, a large energy difference between the two bands reduces the excitation probability.

Pristine β_{12}-borophene is a metal, although we can change the electronic phase by applying an electric field. According to Fig. 5 and 6 it is clear that the band gap increases with EEF in all Hamiltonian models. The band gap in the pristine homogeneous model is zero, but when the voltage increases, gap opening occurs. For $V = 3$ eV the gap of the homogeneous model is about 0.15 eV and with increasing the electric field to $V = 5$ eV the gap increases to 0.5 eV. For the pristine case in the inversion non-symmetric mode, there is a gap of about 0.254 eV which increases with an electric field to ε0.317 eV and 0.6 eV for $V = 3$ eV and $V = 5$ eV respectively. Finally, the β_{12}-borophene monolayer in the pristine inversion symmetric model is gapless and for $V = 3$ eV and $V = 5$ eV the band gap arrives at 0.02 eV and 0.3 eV energies respectively.

In the present work, for inter-band transitions, the Fermi energy (E_F) locates at the midgap between the conduction and valence bands at the K' (or K) point. Also, because of momentum conservation, we considered only direct inter-band transitions ($q \rightarrow 0$) where q indicates the wave-vector change before and after the scattering process. So we neglect indirect transitions and consider two direct transitions between both valences and three conduction bands.

The maximum in the real part of optical conductivity along the x-direction ($\Re\sigma_{xx}$) in all three models represents the gap. Fig. 7 shows the real and imaginary parts of the optical conductivity along the x-direction for the inversion non-symmetric model. According to the plots, in the pristine case, in the real part, there is a peak at energy $\varepsilon = 0.26$ eV, which is equal to the band gap of the pristine inversion non-symmetric model. When we apply an EEF equal to $V = 3$ eV to β_{12}-borophene, the peak of the real part of the optical conductivity shifts toward higher energies, which is known as blue shift. At this voltage, the peak energy is equal to the band gap and is about 0.317 eV. Also, by applying an electric field $V = 5$ eV, this peak is located at $\varepsilon = 0.6$ eV. According to the Kramers–Kronig relation, dips in the imaginary part are at an energy equal to the peak in the real part.

As mentioned earlier, the band gap for the inversion-symmetric model in the pristine case is zero. According to

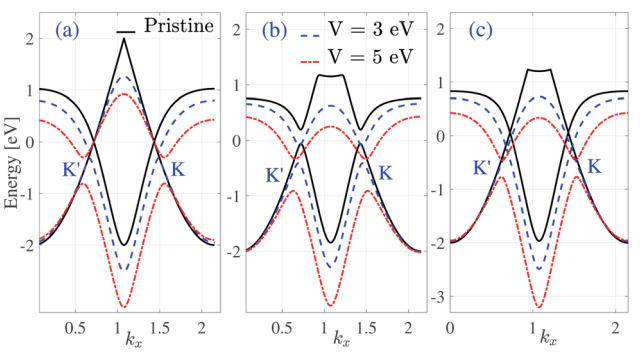

Fig. 5 Band structure of β_{12}-borophene in the vicinity of the K' and K points for the (a) homogeneous (b) inversion non-symmetric and (c) inversion symmetric models in $k_y = 0$ in the presence of an EEF.

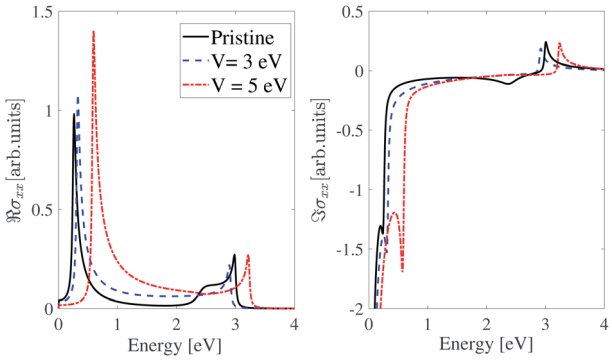

Fig. 7 Real and imaginary parts of the IOC of polarized light along the x-direction for the inversion non-symmetric model of β_{12}-borophene in the presence of an electric field.

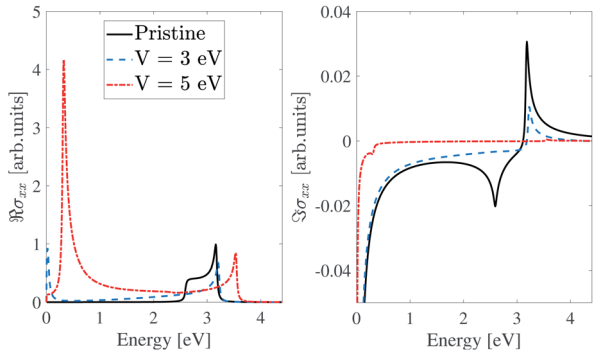

Fig. 8 Real and imaginary parts of the IOC of polarized light along the x-direction for the inversion symmetric model of β_{12}-borophene in the presence of an electric field.

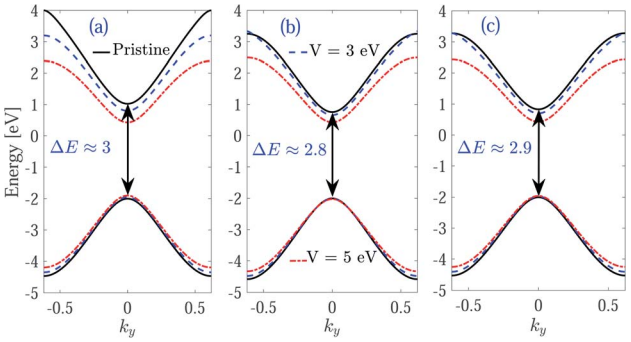

Fig. 10 An overview of the lowest conduction band and the highest valence band at $k_x = 0$ under an EEF for (a) homogeneous (b) inversion non-symmetric and (c) inversion symmetric models.

Fig. 8 when we applied an electric field equal to $V = 3$ eV to β_{12}-borophene, a peak appeared in the real part of optical conductivity at an energy of about 0.02 eV that is equal to the β_{12}-borophene band gap at $V = 3$ eV. Applying an EEF $V = 5$ eV to β_{12}-borophene leads to shifting the peak of the $\Re\sigma_{xx}$ to $\varepsilon = 0.3$ eV which is consistent with the band gap.

As we see in Fig. 9 due to the zero-gap for the homogeneous model in the pristine case, there is no peak in the real part of optical conductivity at low energies. But by applying an EEF, the band gap opening occurs, and at $V = 3$ eV and $V = 5$ eV the band gap reaches $\varepsilon = 0.15$ eV and $\varepsilon = 0.5$ eV respectively, and peaks appear at these energies. Also, according to the Kramers–Kronig relation, there is a dip in the imaginary parts at these energies.

Due to the anisotropic behavior of β_{12}-borophene, the effect of the EEF on the optical conductivity in the y-direction (σ_{yy}) is less than that in the x-direction. As shown in Fig. 10, the β_{12}-borophene band structure at $k_x = 0$ and $-\pi/\sqrt{3}a \leq k_y \leq \pi/\sqrt{3}a$ behaves differently compared to Fig. 5. So we expect the IOC to be different for polarized light along the y-direction. In the IOC for light polarized along the y-direction in the pristine case, peaks and dips appear at the energies shown in Fig. 10, and this is so-called anisotropic optical conductivity. Therefore, we expect the peaks in $\Re\sigma_{yy}$ to be at $\varepsilon = 3.0$ eV, 2.80 eV and 2.90 eV for the pristine homogeneous, inversion non-symmetric and inversion symmetric models respectively. The use of an EEF also reduces the energy difference between the highest valence and the lowest conduction band at $k_x = 0$, so peaks and dips of the IOC shift to lower energies.

As shown in Fig. 11, the EEF has no significant effect on the optical conductivity of the inversion-symmetric model for light polarized along the y-direction. As we expect from Fig. 10, in the pristine case the optical conductivity peak is at $\varepsilon = 2.9$ eV, and by applying an EEF, the optical conductivity plot shifts toward lower energies (redshift) and for $V = 3$ eV and $V = 5$ eV the peak of the real part of the IOC shifts to $\varepsilon = 2.7$ eV and 2.4 eV respectively.

The imaginary and real parts of the optical conductivity of the inversion non-symmetric model for polarized light along the y-direction are shown in Fig. 12. Like the inversion-symmetry model, the EEF has little effect on the optical conductivity in the y-direction. Peaks of the real parts of optical conductivity in the pristine and perturbed cases with $V = 3$ eV and $V = 5$ eV, are at $\varepsilon = 2.8$ eV, 2.7 eV and 2.5 eV respectively, and there are similar situations for the imaginary parts.

As illustrated in Fig. 13 in the homogeneous model, the effects of an EEF on σ_{yy} are similar to the inversion-symmetric

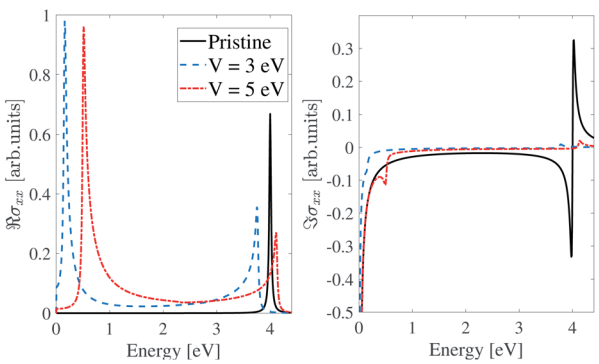

Fig. 9 Real and imaginary parts of the IOC of polarized light along the x-direction for the homogeneous model of β_{12}-borophene in the presence of an electric field.

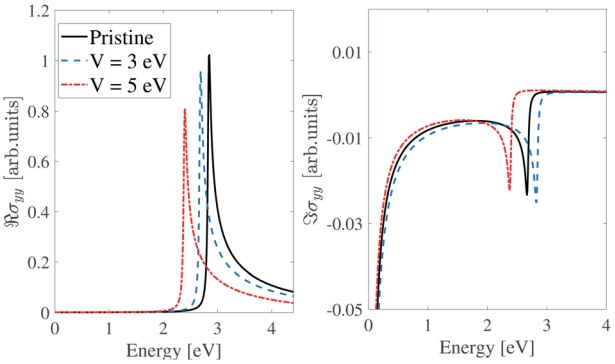

Fig. 11 Real and imaginary parts of the IOC of the inversion symmetric model of β_{12}-borophene for polarized light along the y-direction in the presence of an electric field.

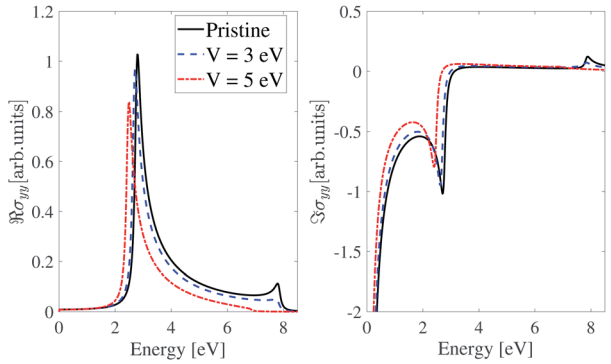

Fig. 12 Real and imaginary parts of the IOC of the inversion non-symmetric model of β_{12}-borophene for polarized light along the y-direction in the presence of an electric field.

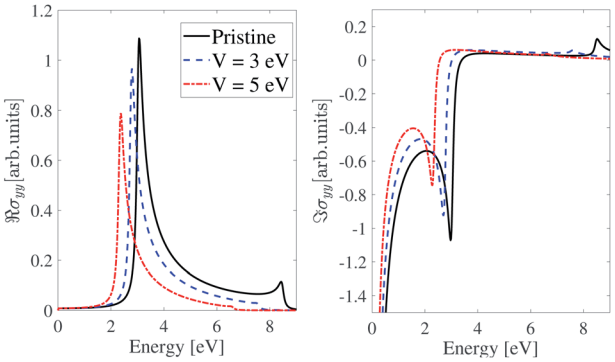

Fig. 13 Real and imaginary parts of the IOC of the homogeneous model of β_{12}-borophene for polarized light along the y-direction in the presence of an electric field.

and inversion non-symmetric models. The maximum value of $\Re\sigma_{yy}$ in the pristine case is at $\varepsilon \simeq 3.0$ eV and for the electric field-induced case, real part of σ_{yy} shifts toward lower energies and experiences a redshift. The peaks energies for $V = 3$ eV and $V = 5$ eV are at $\varepsilon = 2.8$ eV and 2.4 eV respectively.

At the low energies in the THz region, intra-band transitions exceed the inter-band term (both real and imaginary parts), whereas, in the high-frequency, this term does not play an important role in the optical conductivity. Fig. 14 shows the real and imaginary parts of the intra-band optical conductivity of β_{12}-borophene at the Fermi energy $E_F = E_c(K') + \mu_c$ for light polarized along y-direction. Due to the similarity of the intra-band optical conductivity for light polarized along x and y-directions, real and imaginary parts of σ_{xx} are absent in this work. Our results show a similarity between the intra-band optical conductivity of β_{12}-borophene and graphene.[30] As we can see in Fig. 14 the height of the $\Re\sigma_{yy}$ and $\Im\sigma_{yy}$ is reduced by applying an EEF, and there is no energy shifting in the real and imaginary parts of the optical conductivity.

In the end, our results show the anisotropic behavior of the β_{12}-borophene due to the anisotropic band structure. For DC currents ($\omega \rightarrow 0$) optical conductivity converts to electrical conductivity. In a study by Khoa *et al*[23] electrical conductivity of

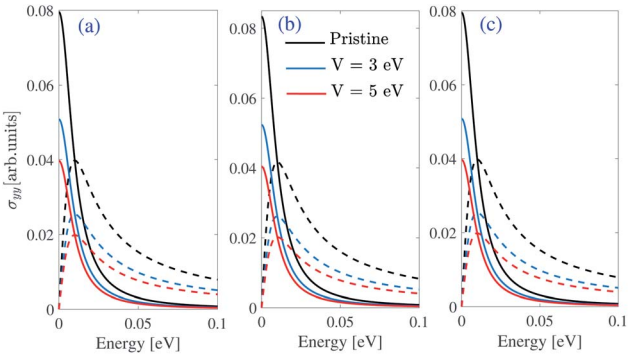

Fig. 14 Real (solid lines) and imaginary (dashed lines) parts of the intra-band optical conductivity polarized along the y-direction by chemical potential $\mu_c = 0.5$ eV and $E_F = \mu_c + E_c(K')$ of (a) homogeneous (b) inversion non-symmetric and (c) inversion symmetric models of β_{12}-borophene in the presence of an EEF where $E_c(K')$ is the conduction band energy at the K' point.

impurity-induced and gated β_{12}-borophene was calculated, and similar to our results, they also reported anisotropic electrical conductivity. Phosphorene has an anisotropic behavior as a puckered 2D material. In a study on the optical properties of strained phosphorene, this anisotropy was observed in the absorption and refraction coefficients.[27] Therefore, anisotropic behavior in optical conductivity of β_{12}-borophene is predictable, as we have reported in the present work.

4 Conclusions

In summary, for the β_{12}-borophene monolayer, both the band gap and the optical conductivity can be modified using an EEF. In all three models, the gap increases by applying an electric field. The anisotropic band structure of β_{12}-borophene leads to different optical conductivity for light polarized along the x and y-directions. Also, the peak of the real part of optical conductivity along the x-direction reflects the band gap, and as the electric field increases, it shifts to higher energies and experiences a blue shift. In contrast to σ_{xx}, by applying an electric field to β_{12}-borophene, the optical conductivity in the y-direction was shifted to lower energies, and a redshift occurred. Also, intra-band optical conductivity behavior is similar to that of graphene, and applying an external electric field does not shift plots to lower or higher energies but only reduces the height of the IOC plots.

Conflicts of interest

There are no conflicts to declare.

Notes and references

1 K. S. Novoselov, A. K. Geim, S. V. Morozov, D. Jiang, Y. Zhang, S. V. Dubonos, I. V. Grigorieva and A. A. Firsov, *Science*, 2004, **306**, 666–669.

2 A. J. Mannix, X.-F. Zhou, B. Kiraly, J. D. Wood, D. Alducin, B. D. Myers, X. Liu, B. L. Fisher, U. Santiago, J. R. Guest,

M. J. Yacaman, A. Ponce, A. R. Oganov, M. C. Hersam and N. P. Guisinger, *Science*, 2015, **350**, 1513–1516.
3 Z. Zhang, A. J. Mannix, X. Liu, Z. Hu, N. P. Guisinger, M. C. Hersam and B. I. Yakobson, *Sci. Adv.*, 2019, **5**, eaax0246.
4 B. Feng, J. Zhang, R.-Y. Liu, T. Iimori, C. Lian, H. Li, L. Chen, K. Wu, S. Meng, F. Komori and I. Matsuda, *Phys. Rev. B*, 2016, **94**, 041408.
5 Y. Liu, E. S. Penev and B. I. Yakobson, *Angew. Chem., Int. Ed.*, 2013, **52**, 3156–3159.
6 Z. Zhang, Y. Yang, G. Gao and B. I. Yakobson, *Angew. Chem.*, 2015, **127**, 13214–13218.
7 B. Peng, H. Zhang, H. Shao, Z. Ning, Y. Xu, G. Ni, H. Lu, D. W. Zhang and H. Zhu, *Mater. Res. Lett.*, 2017, **5**, 399–407.
8 A. P. Sergeeva, I. A. Popov, Z. A. Piazza, W.-L. Li, C. Romanescu, L.-S. Wang and A. I. Boldyrev, *Acc. Chem. Res.*, 2014, **47**, 1349–1358.
9 L.-S. Wang, *Int. Rev. Phys. Chem.*, 2016, **35**, 69–142.
10 H. Li, I. E. Castelli, K. S. Thygesen and K. W. Jacobsen, *Phys. Rev. B: Condens. Matter Mater. Phys.*, 2015, **91**, 045204.
11 M. Ezawa, *Phys. Rev. B*, 2017, **96**, 035425.
12 P. T. T. Le, T. C. Phong and M. Yarmohammadi, *Phys. Chem. Chem. Phys.*, 2019, **21**, 21790–21797.
13 M. H. Evans, J. Joannopoulos and S. T. Pantelides, *Phys. Rev. B: Condens. Matter Mater. Phys.*, 2005, **72**, 045434.
14 B. Feng, O. Sugino, R.-Y. Liu, J. Zhang, R. Yukawa, M. Kawamura, T. Iimori, H. Kim, Y. Hasegawa, H. Li, *et al.*, *Phys. Rev. Lett.*, 2017, **118**, 096401.
15 H. Tang and S. Ismail-Beigi, *Phys. Rev. B: Condens. Matter Mater. Phys.*, 2010, **82**, 115412.
16 X. Wu, J. Dai, Y. Zhao, Z. Zhuo, J. Yang and X. C. Zeng, *ACS Nano*, 2012, **6**, 7443–7453.
17 E. S. Penev, S. Bhowmick, A. Sadrzadeh and B. I. Yakobson, *Nano Lett.*, 2012, **12**, 2441–2445.
18 C. Ozdogan, S. Mukhopadhyay, W. Hayami, Z. Guvenc, R. Pandey and I. Boustani, *J. Phys. Chem. C*, 2010, **114**, 4362–4375.
19 H. Tang and S. Ismail-Beigi, *Phys. Rev. B: Condens. Matter Mater. Phys.*, 2010, **82**, 115412.
20 H. Zhou, Y. Cai, G. Zhang and Y.-W. Zhang, *npj 2D Mater. Appl.*, 2017, **1**, 1–7.
21 E. S. Penev, A. Kutana and B. I. Yakobson, *Nano Lett.*, 2016, **16**, 2522–2526.
22 A. A. Kistanov, Y. Cai, K. Zhou, N. Srikanth, S. V. Dmitriev and Y.-W. Zhang, *Nanoscale*, 2018, **10**, 1403–1410.
23 D. Q. Khoa, N. N. Hieu and B. D. Hoi, *Phys. Chem. Chem. Phys.*, 2020, **22**, 286–294.
24 L. Adamska and S. Sharifzadeh, *ACS Omega*, 2017, **2**, 8290–8299.
25 X. Zhang, J. Hu, Y. Cheng, H. Y. Yang, Y. Yao and S. A. Yang, *Nanoscale*, 2016, **8**, 15340–15347.
26 B. Peng, H. Zhang, H. Shao, Y. Xu, R. Zhang and H. Zhu, *J. Mater. Chem. C*, 2016, **4**, 3592–3598.
27 M. Yarmohammadi, M. Mortezaei, T. S. Tien and L. T. T. Phuong, *J. Phys.: Condens. Matter*, 2020, **32**, 465301.
28 C. H. Yang, J. Y. Zhang, G. X. Wang and C. Zhang, *Phys. Rev. B*, 2018, **97**, 245408.
29 I. Kupčić, *Phys. Rev. B: Condens. Matter Mater. Phys.*, 2009, **79**, 235104.
30 Y. V. Bludov, N. M. Peres and M. I. Vasilevskiy, *J. Opt.*, 2013, **15**, 114004.